Agricultural Water Management 150 (2015) 67–80

Contents lists available at ScienceDirect

Agricultural Water Management

journal homepage: www.elsevier.com/locate/agwat

Field analysis of water and nitrogen fate in lowland paddy fields under different water managements using HYDRUS-1D

Xuezhi Tan[a,b], Dongguo Shao[a,*], Wenquan Gu[a], Huanhuan Liu[a]

[a] State Key Laboratory of Water Resources and Hydropower Engineering Science, Wuhan University, Wuhan, 430072, PR China
[b] Department of Civil and Environmental Engineering, University of Alberta, Edmonton, AB, Canada T6G 2W2

ARTICLE INFO

Article history:
Received 18 February 2014
Accepted 2 December 2014
Available online 18 December 2014

Keywords:
Alternate wetting and drying (AWD)
Continuously flooded (CF)
Lowland paddy fields
Soil water
N transformations
HYDRUS-1D

ABSTRACT

With the wide adoption of alternate wetting and drying (AWD) irrigation for rice production, the water and nitrogen (N) fate in lowland paddy fields under AWD irrigation was needed to be investigated for assessing the water saving and environmental effects of AWD, compared to traditional continuously flooded (CF) irrigation. The HYDRUS-1D software package was used to simulate water movement, and N transport and transformations in experimental paddy fields under AWD and CF irrigation during 2007 and 2008. The variation in N transformation between AWD and CF paddy fields due to different water regimes in soil profiles were represented by time-varying boundary conditions and N transformation parameters that are dependent on soil water content. Simulations show that AWD irrigation decreased 27.8 and 19.0% of percolation, 5.0–11.2% and 3.0–23.5% of N leaching losses in 2007 and 2008, respectively, compared to CF irrigation. However, AWD irrigation increased 6.0–22.0% and 2.5–11.7% of N losses of volatilization, and 6.3–9.4% and 4.5–7.6% of nitrification, as well as 6.7–19.8% and 4.1–11.2% of denitrification in 2007 and 2008, respectively. These results reflect the intensified nitrification–denitrification processes that were caused by the relatively high ammonium concentration, and alternate aerobic and anaerobic environment in AWD paddy fields. The increased nitrate, which was formed from nitrification of ammonium in drying (aerobic) phase, can be easily denitrified to N_2 or N_2O in the wetting (anaerobic) phase. Therefore, the practice of AWD irrigation should consider its side effects on increasing N emissions from paddy fields that may also decrease the N use efficiency. Simulation of water and N regime together using HYDRUS-1D is an alternative system approach to improve water and N management for sustainable rice production.

1. Introduction

Water and nitrogen (N) are two of the most important inputs for high grain yields in rice production. Rice is a heavy water consumer, but water for rice production is increasingly becoming scarce and expensive due to the increasing demand for water from the ever-growing population, competition for water from other sectors, such as urbanization, tourism industry and ecosystem services (Roost et al., 2008). Therefore, various water-saving irrigation (WSI) techniques have been introduced to replace traditional continuously flooded (CF) irrigation for achieving high water-efficient irrigation in rice production (Li and Barker, 2004). The most widely adopted WSI is the alternate wetting and drying (AWD) irrigation that is also referred to as alternately submerged and nonsubmerged irrigation (Belder, 2004; Cabangon et al., 2011; Cabangon et al., 2004; Moya et al., 2004; Tan et al., 2013, 2014; Yao et al., 2012). As lowland paddy fields are being transited from CF to AWD irrigation, the pathways and amount of water and N losses in lowland paddy fields may change due to the difference of water and N regime in paddy fields under AWD and CF irrigation.

Evaluation of the water and N fate in lowland paddy fields is complicated because of many pathways of water losses and N transformation processes that occur in flooded or non-flooded conditions. Field condition of alternate wetting (anaerobic) and drying (aerobic) increases the complexity of water movement and N transformation in paddy fields, compared to the condition of continuously flooded (anaerobic) or continuously non-flooded (aerobic) conditions. A large number of reported results indicate that AWD decreases the water input and enhances the water productivity for rice production (Belder, 2004; Bouman et al., 2007; Moya et al., 2004; Zhang et al., 2008). However, the transport and transformations of N applied to paddy fields under AWD irrigation are not well understood, although some field experiments showed the effects of AWD irrigation on N use in paddy fields (Lin et al., 2006; Sun et al., 2012; Zhang et al., 2009).

* Corresponding author. Tel.: +86 13986298750.
E-mail address: dgshao1@gmail.com (D. Shao).

http://dx.doi.org/10.1016/j.agwat.2014.12.005
0378-3774/

Much attention has been given on N losses that decrease the N use efficiency and cause serious environmental problems. Several field measurements were conducted to study the N fate and environmental consequences of paddy fields under different field conditions, e.g., rice-wheat rotations (Zhao et al., 2009), N applications with different rates (Kyaw et al., 2005; Zhou et al., 2008), and WSI practices (Belder et al., 2005; Patil and Das, 2013). However, these measurements were hard to show the N transformations, although Kyaw et al. (2005) had combined laboratory estimations of N fixation and denitrification. N losses in paddy fields under AWD irrigation can be extremely large compare to that under CF irrigation, because of the differences in N transformations between anaerobic and aerobic environments. Nitrate (NO_3^-—N) formed by nitrification of ammonium (NH_4^+—N) during the drying days can be quickly lost by denitrification in the following wetting days (Buresh et al., 2008). It is difficult to accurately estimate the amount of N transformed in paddy fields by laboratory simulated experiments as the experimental conditions cannot be fully controlled as the real dynamic field conditions.

Modeling approach for the water and N balances in lowland paddy fields is a potential alternative to improve the performance of WSI for rice production, although it is of great challenge as water and N processes relate to the agrometeorological conditions, soil properties, rice growth and water regime in specific paddy fields. Antonopoulos (2010) conceptually coupled the water and N balances, respectively, for flooded water layer and soil layer. Simulation models, e.g., RICEWQ (Williams et al., 1998), PADDY (Inao and Kitamura, 1999), PCPF-1 (Watanabe et al., 2006), PADDIMOD (Jeon et al., 2005), mainly focused on the nutrient and pesticide balance of flooded water and surface soil layers. They were not applicable to the paddy fields under AWD. So far several Darcy-law driven one dimensional models, e.g., SAWAH (ten Berge et al., 1995), ORYZA (Bouman et al., 2001; Feng et al., 2007; Yadav et al., 2011), SWMS (Tournebize et al., 2006), HYDRUS (Garg et al., 2009; Janssen and Lennartz, 2009; Sander and Gerke, 2009; Tan et al., 2014), have been employed to simulate water movement in paddy fields, and to explore water management options for best practice of WSI as well. However, to our knowledge, these models were seldom used to simulate the N transport and transformations in paddy fields, especially AWD fields.

Lowland paddy soils present structured and stratified layers, typically consisting of top puddled layer, hardpan layer, and underlying subsoil layer. The compaction of plow pan is the key to determine the water and solution transferring capability, while the conductivity in plow pan is the key for water and solution movement in the whole profile of paddy fields (Tournebize et al., 2006; Patil et al., 2011). It is needed to understand the differences of water and N distributions in lowland soil profiles between paddy fields under AWD and CF irrigation for better practice of AWD irrigation. HYDRUS (Simunek et al., 2008) have been widely used to analyze the multi-layer soil water flow in paddy fields for preferential flow (Dash et al., 2014; Garg et al., 2009; Sander and Gerke, 2009; Tan et al., 2014), seepage across paddy fields bunds (Janssen and Lennartz, 2009), and heavy metal transport (Nguyen Ngoc et al., 2009). However, transport and transformations of N or other decayed chemicals in paddy fields were seldom investigated by HYDRUS modeling (Patil and Das, 2013), although it was popularly used for the analysis of N transport and transformations in dry land fields cultivated with other crops, such as maize (Crevoisier et al., 2008; Ramos et al., 2011; Ramos et al., 2012), wheat (Wang et al., 2010), onion (Ajdary et al., 2007), and corn (Mailhol et al., 2007).

The objective of this study was to use the HYDRUS-1D software package to evaluate N transport and transformations in paddy fields by analyzing experimental data collected in split-plot designed field experiments (Tan et al., 2013) with AWD and CF irrigation treatments. The effects of AWD on the water and N fate were further evaluated by the HYDRUS-1D simulation results through comparing the water and N balance components of paddy fields under AWD and CF irrigation.

2. Materials and methods

2.1. Field experiment

As the field experimental data used in this study was described in detail by Tan et al. (2013), here, we have given relevant information that was highly associated with this HYDRUS-1D modeling study.

2.1.1. Experimental fields

Field experiment was conducted at the Tuanlin experimental paddy fields of Hubei, China (30° 49′N, 112° 10′E) for irrigation science, which were extensively researched for WSI practices including AWD (Belder et al., 2005; Cabangon et al., 2004; Li and Barker, 2004; Tan et al., 2014). Experiment was conducted during the rice growing season (May to September) of 2007 and 2008. The local average altitude and temperature is 90 m and 16 °C, respectively. It belongs to the zone of subtropical monsoon climate in terms of climatic regionalization. The rainfall and pan evaporation amounts to 700–1100 mm and 1300–1800 mm, respectively. Irrigation and drainage experiments were carried out in 24 plots (9×8 m, Fig. 1). The concrete block levees of paddy plots were lined with plain sheets extending downward about 50-cm deep to prevent lateral seepage across plots. Table 1 shows the basic chemical property of soils from experimental paddy plots.

2.1.2. Water and N treatments

The experiments were laid out in a split-plot design with water as main blocks and N fertilizer as sub-blocks with four replicates. The experiments had two irrigation treatments, AWD and CF, and three N fertilizer treatments for each irrigation treatment, low N (LN, 0 kg ha^{-1}), medium N (MN, 135 kg ha^{-1}), and high N (HN, 180 kg ha^{-1}). The controlled thresholds of soil water content in different rice growth stages after turning green, which is within 65–80% of saturated water content, for triggering AWD irrigation are referred to Tan et al. (2013). Paddy plots under CF irrigation were maintained ponded water during the rice growing season, except during the growth stage of late tillering and yellow ripening when rice needs little water. In CF paddy plots, irrigation was conducted when the paddy ponded water depth was lower than the lower depth limit designed for specific rice growth stage that was shown in Table 2 of Tan et al. (2013). N fertilizer of two levels was applied as urea in three splits: 50% for basal application (June-5-2007 and June-1-2008), 30% at tillering (July-2-2007 and June-29-2008) and 20% at panicle initiation (July-25-2007 and July-21-2008). Six treatments combining two water managements and three N managements were AL (AWD and LN), AM (AWD and MN), AH (AWD and HN), CL (CF and LN), CM (CF and MN), and CH (CF and HN) (Fig. 1). All twenty-four experimental paddy plots were conducted with the same crop management, e.g., P, K fertilization, and pesticide application. They were left fallow over the off crop season. Before rice planting (June-6-2007 and June-2-2008), plots were traditionally flooded to puddle by two passes of rotary plow about 18 cm deep, and leveled for the cultivation.

2.1.3. Field measurements and analysis

The meteorological data were collected by the Tuanlin Weather Station that was 100 m away from the experimental paddy plots. In each plot, TDR (time domain reflectometer) probes were used to measure soil water contents at depth of 33 and 58 cm, and the

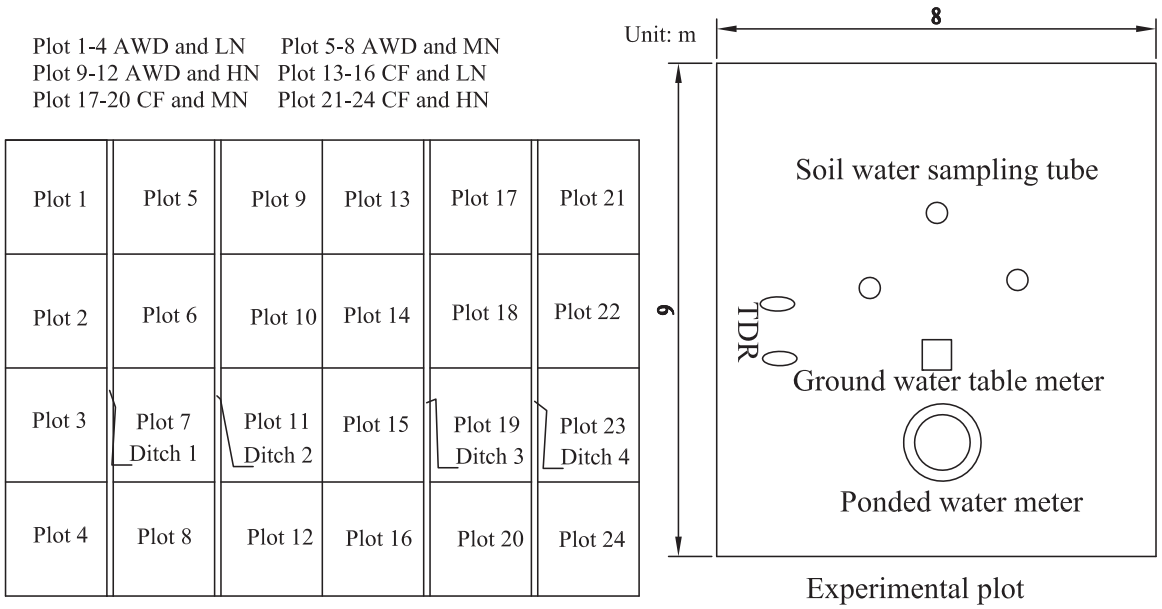

Fig. 1. Schematic of the field layout and locations of instruments, AWD and CF are water treatments, and LN (low N, 0 kg ha^{-1}), MN (medium N, 135 kg ha^{-1}), and HN (high N, 180 kg ha^{-1}) are N treatments.

Table 1
Basic chemical property of soils from experimental paddy plots.

Soil layer	pH	Organic matter (%)	Total N (g kg^{-1})	NH_4^+—N (mg kg^{-1})	NO_3^-—N (mg kg^{-1})
Cultivated horizon (0–18 cm)	5.8(4)[a]	25.31(18)	1.33(28)	4.28(23)	7.34(24)
Plow pan (18–33 cm)	5.6(6)	22.44(23)	1.16(25)	3.95(36)	8.21(27)
Illuvial horizon (33–100 cm)	5.6(3)	7.32(12)	0.93(13)	2.18(9)	2.85(26)

[a] Values in the parenthesis indicate the coefficients of variation (CV) expressed in percentage.

ponded water depth and groundwater table was, respectively, measured by the ponded water meter and groundwater table meter that were made by PVC tubes. Tan et al. (2013) and Tsubo et al. (2005) described these measuring instruments in detail. The ponded water level in wetting days or soil water content in drying days, as well as groundwater table were observed and recorded manually every day at 2:00 pm during rice growing seasons.

The daily values of the reference evapotranspiration rate (ET_0) were calculated using the Penman–Monteith equation (Allen et al., 1998). Rice potential evapotranspiration rates (ET_c) were then calculated by multiplying ET_0 by rice coefficient (K_c) that accounts the soil evaporation and rice transpiration. Values of K_c at different rice growth stage were taken from Allen et al. (1998) and Tyagi et al. (2000). With ET_c, potential evaporation E_p was calculated using the equation (Pachepsky et al., 2004):

$$E_p = ET_c \times \exp^{-\beta LAI} \quad (1)$$

where β is the radiation extinction coefficient and LAI is the leaf area index. The β value for rice was taken as 0.3 as Phogat et al. (2010) calibrated. Note that the leaf area index was not measured for the division of ET_0 daily values into potential crop transpiration T_p and E_p. Since there was no significant grain yields variation between AWD and CF paddy fields (Tan et al., 2013), we used the LAI values measured by Phogat et al. (2010) in different growth stage under no salinity and N (180 kg ha^{-1}) stress for both AWD and CF paddy fields. The LAI values for the paddy plots with N fertilization of 0 and 135 kg ha^{-1} were assumed to be proportional to that of the paddy plots with N fertilization of 180 kg ha^{-1} by their measured rice yields.

Ceramic cups were installed at soil depth of 33 and 58 cm to collect soil water using a vacuum pump once a week. Ponded water and groundwater were sampled as well for N analysis. Sampled soil water was analyzed in laboratory for the concentrations of NH_4^+—N and NO_3^-—N.

2.2. Model simulation using HYDRUS-1D

Since the seepage in paddy plots was minimized and the water and solute flow can be simplified to the vertical movement, the HYDRUS-1D software package (Simunek et al., 2008) was used to simulate one-dimensional water flow and N transport and transformations in the experimental plots. The simulation of water flow is following our previous work on other experiment data (Tan et al., 2014), while the N transport and transformations innovatively simulated in this study. The solute transport module was run to simulate N concentrations of urea, NH_4^+—N and NO_3^-—N in soil profile.

2.2.1. Water flow

The governing flow equation for variably saturated soil water movement is given by the Richards' equation:

$$\frac{\partial \theta}{\partial t} = \frac{\partial}{\partial Z}\left[K(h)\left(\frac{\partial h}{\partial Z} + 1\right)\right] - S(Z,t) \quad (2)$$

where θ is the volumetric soil water content ($L^3\,L^{-3}$), t is the time (T^{-1}), h is the soil water pressure head (L), Z is the vertical space coordinate (L), K is the hydraulic conductivity function ($L\,T^{-1}$), S is the sink term representing water uptake by rice roots ($L^3\,L^{-3}\,T^{-1}$). We used van Genuchten's K–h and θ–h relationships

(van Genuchten, 1980) for describing soil hydraulic properties of lowland paddy soils:

$$\theta(h) = \theta_r + \frac{\theta_s - \theta_r}{\left[1 + (\alpha h)^n\right]^m}, \quad h \le 0 \tag{3}$$

$$K(h) = K_s S_e^l \left(1 - \left(1 - S_e^{1/m}\right)^m\right)^2$$

with

$$m = 1 - \frac{1}{n} \quad \text{and} \quad S_e = \frac{\theta - \theta_r}{\theta_s - \theta_r} \tag{4}$$

where θ_r and θ_s denotes the residual and saturated volumetric water contents ($L^3\,L^{-3}$), respectively; α (L^{-1}), m (−) and n (−) are fitting parameters of soil water characteristic curve; l (−) is the pore connectivity parameter (=0.5); K_s ($L\,T^{-1}$) is the saturated hydraulic conductivity and S_e (−) is the relative saturation.

2.2.2. Rice root water uptake

Actual rice root water uptake, the sink term, S, in the Eq. (2) was estimated using the general model introduced by Feddes et al. (1978), which was coupled in HYDRUS-1D package. The potential transpiration rate, $T_P(t)$ ($L\,T^{-1}$), was assumed to be exponentially distributed, $\beta(Z,t)$ (L^{-1}), over the rice root zone, the actual volumes of water removed from unit volume of soil per unit of time, $S(h,Z,t)$ ($L^3\,L^{-3}\,T^{-1}$), can be derived considering the water and osmotic stresses (Feddes et al., 1978; Šimůnek and Hopmans, 2009):

$$S(h,Z,t) = \beta(Z,t)\,\alpha(h)\,T_P(t) \tag{5}$$

where $\alpha(h)$ is the dimensionless function of the soil water pressure head in response to water stress, taking values between 0 and 1. We used the Feddes' model (Feddes et al., 1978) for $\alpha(h)$ by a piecewise linear reduction function parameterized by four critical values of the water pressure head ($h_4 < h_3 < h_2 < h_1$) to describe the multiplicative water and osmotic stress to the rice root water uptake.

$$\alpha(h) = \begin{cases} \dfrac{h - h_4}{h_3 - h_4} & h_3 > h > h_4 \\ 1 & h_2 \ge h \ge h_3 \\ \dfrac{h - h_4}{h_3 - h_4} & h_1 > h > h_2 \\ 0 & h \le h_4 \quad \text{or} \quad h \ge h_1 \end{cases} \tag{6}$$

The threshold parameters in rice root water uptake model were, respectively, set to be h_1 = 100 cm, h_2 = 55 cm, h_3 (high) = −250, h_3 (low) = −160 cm and h_4 = −15,000 cm. These critical pressure head values were optimized by Singh et al. (2003, 2006) and also used by Phogat et al. (2010) for rice water uptake simulation.

There was no salinity stress because of the low salinity in paddy plots. Thus, the actual transpiration rate can be calculated by integrating Eq. (5) over the whole root domain L_R:

$$ET_a = \int_{L_R} S(h,Z,t)\,dZ = T_P(t) \int_{L_R} \alpha(h)\,\beta(Z,t)\,dZ \tag{7}$$

The root domain L_R was described by the variable root depth grow model (Simunek et al., 2008; Šimůnek and Suarez, 1993) included in HYDRUS-1D:

$$L_R(t) = L_m f_r(t) \tag{8}$$

where L_m is the maximum rooting depth (L); $f_r(t)$ is a dimensionless rooting growth coefficient, which was estimated by Verhulst–Pearl logistic growth function:

$$f_r(t) = \frac{L_0}{L_0 + (L_m - L_0)\,e^{-rt}} \tag{9}$$

where L_0 is the initial value of the rooting depth at the beginning of the growing season (L), and r the growth rate (T^{-1}), which was calculated from the measured rooting depth data. Parameters for root growth model in this study were set to 10 cm for L_0 in both paddy plots under AWD and CF irrigation, while 60 and 50 cm for L_m in paddy plots under AWD and CF irrigation, respectively. The measured rooting depth of paddy plots under AWD (60 cm) was higher than that under CF (50 cm) irrigation, as rice stimulated the root downward growth to obtain enough water uptake under water stress that rice encountered in paddy plots under AWD irrigation. The measured root depth data (32 cm in AWD plots and 28 cm in CF plots) at the DAT = 40 was used to calculate rice growth rate.

2.2.3. Nitrogen transport and transformations

The partial differential equations governing one-dimensional advective–dispersive N transport and transformations in variably-saturated paddy soils are taken as:

Urea:

$$\frac{\partial \theta c_{w,1}}{\partial t} = \frac{\partial}{\partial Z}\left(\theta D_1 \frac{\partial c_{w,1}}{\partial Z}\right) - \frac{\partial q c_{w,1}}{\partial Z} - \mu'_{w,1}\theta c_{w,1} \tag{10}$$

NH_4^+—N:

$$\frac{\partial \theta c_{w,2}}{\partial t} + \rho \frac{\partial c_{s,2}}{\partial t} = \frac{\partial}{\partial Z}\left(\theta D_2 \frac{\partial c_{w,2}}{\partial Z}\right) - \frac{\partial q c_{w,2}}{\partial Z} + \mu'_{w,1}\theta c_{w,1} - \left(\mu_{w,2} + \mu'_{w,2}\right)\theta c_{w,2} - \left(\mu_{s,2} + \mu'_{s,2}\right)\rho c_{s,2} + \gamma_{w,2}\theta + \gamma_{s,2}\rho - S(Z,t)\,c_{w,2} \tag{11}$$

NO_3^-—N:

$$\frac{\partial \theta c_{w,3}}{\partial t} = \frac{\partial}{\partial Z}\left(\theta D_3 \frac{\partial c_{w,3}}{\partial Z}\right) - \frac{\partial q c_{w,3}}{\partial Z} + \mu'_{w,2}\theta c_{w,2} + \mu'_{s,2}\rho c_{s,2} - \left(\mu_{w,3} + \mu_{s,3}\right)\theta c_{w,3} - S(Z,t)\,c_{w,3} \tag{12}$$

where subscript number 1, 2 and 3 denotes the N species, i.e., urea, NH_4^+—N and NO_3^-—N, respectively, and w and s is the liquid and solid phase of N. c is the N concentration ($M\,M^{-1}$), ρ is the soil bulk density ($M\,L^{-3}$), D is the N dispersion coefficient ($L^2\,T^{-1}$), q is the volumetric water flux ($L\,T^{-1}$), μ represents the first-order N transformation rate constant (T^{-1}), while μ' is the similar first-order rate constant providing connections between urea, NH_4^+—N and NO_3^-—N, γ is the zero-order N transformation rate constants ($M\,L^{-3}\,T^{-1}$). The dispersion coefficient in the liquid phase D is given by $\theta D = D_L|q| + \theta D_w^0 \tau_w$, where D_w^0 is the molecular diffusion coefficient in free water ($L^2\,T^{-1}$), τ_w is the tortuosity factor in the liquid phase and D_L is the longitudinal dispersivity (L). The last term of Eq. (11) or Eq. (12) is a passive root N uptake. Because of the low absorptivity of paddy soil to urea and NO_3^-—N, so they were simulated only in the liquid phase.

N transformations considered in Eqs. (10)–(12) are hydrolysis, mineralization, fixation, volatilization, nitrification and denitrification in paddy fields (Chowdary et al., 2004; Simunek et al., 2008). Since the dynamics of organic N and biomass in the paddy fields were not simulated in this study, the amount of NH_4^+—N derived from the mieralization and fixation cannot be described by the first-order reactions. In our simulation, the processes of mineralization and fixation, which are very important N sources for rice production (Gaydon et al., 2012), were lumped to be represented

Table 2
Basic physical properties of soils from paddy plots.

Soil layer	ρ_b (g cm^{-3})	θ_f (cm^3 cm^{-3})	Parameters of the water retention equation (van Genuchten model)						
			θ_r (cm^3 cm^{-3})	θ_s (cm^3 cm^{-3})	α (cm^{-1})	n	K_s (cm d^{-1})[b]	K_s (cm d^{-1})[c]	K_s (cm d^{-1})[d]
Cultivated horizon (0–18 cm)	1.33(5)[a]	0.39(14)	0.087(82)	0.502(10)	0.022(34)	1.29(30)	7.83(41)	7.83	7.83
Plow pan (18–33 cm)	1.51(6)	0.32(25)	0.067(73)	0.474(18)	0.013(28)	1.24(20)	0.41(62)	0.45	0.58
Illuvial horizon (33–100 cm)	1.42(3)	0.34(18)	0.062(52)	0.483(15)	0.034(19)	1.41(25)	17.6(35)	17.6	17.6

Note: ρ_b, bulk density; θ_f, field capacity; θ_r, residual volumetric water contents; θ_s, saturated volumetric water contents; α and n, fitting parameters of soil water characteristic curve; K_s, saturated hydraulic conductivity.

[a] Values in the parenthesis indicate the coefficients of variation (CV) expressed in percentage, but we only used the average value of each parameter for soil water modeling.
[b] Measured saturated hydraulic conductivity by soil core analysis.
[c] Calibrated saturated hydraulic conductivity for paddy plots under CF irrigation.
[d] Calibrated saturated hydraulic conductivity for paddy plots under AWD irrigation.

by the zero-order decay chain as $\gamma_{w,2}\theta$ and $\gamma_{s,2}\theta$. The volatilization was represented by the first-order decay chains as $\mu_2\theta c_2$. The nitrification of the NH_4^+—N to NO_3^-—N was calculated by the first-order reactions $\mu'_{w,2}\theta c_{w,2}$ and $\mu'_{s,2}\rho c_{s,2}$ for the N in the liquid and solid phases, respectively. The denitrification was estimated by the first-order decay chains as $\mu_{w,3}\theta c_{w,3}$ and $\mu_{s,3}\rho c_{s,3}$. All these N transformation rate constants were assumed to be dependent on soil water content in the simulation, as AWD irrigation made the soil water regime in paddy fields change a lot during the rice growing season. The water content dependence of degradation coefficients is simulated by equation of (Simunek et al., 2008; Walker, 1974):

$$a\left(\theta\right) = a_r\left(\theta_{\text{ref}}\right)\min\left[1, \left(\frac{\theta}{\theta_{\text{ref}}}\right)^B\right] \tag{13}$$

where a_r is the values of the coefficient at a reference water content θ_{ref}, a is the value at the actual water content θ, and B is a solute dependent parameter (0.7). In this study, the reference water contents $\left(\theta_{\text{ref}}\right)$ for N transformation processes, except denitrification, was regarded as averaged field capacity of three soil layers (Table 2) of each soil layer as Rodrigo et al. (1997) suggested, while θ_{ref} for denitrification was the saturated soil water content.

The process of NH_4^+—N adsorption by soil was accounted by means of linear adsorption isotherms, which relates c_w and c_s in Eq. (8) as follows:

$$c_s = K_d c_w \tag{14}$$

where K_d ($L^3\,M^{-1}$) is the distribution coefficient of NH_4^+—N between liquid and solid phase.

2.2.4. Initial conditions and time-variable boundary conditions

For the simulation of soil water movement in paddy plots, 1 m deep paddy soil domain (Fig. 2) represented the soil columns of experimental paddy plots since the depth of water table to the paddy surface was always lower than 1 m. Initial soil water content of the top layer was the saturated water content (0.502) as the paddy field surface was ponded before rice transplanting. The initial soil water content between the second layer and the bottom layer above the water table were linearly interpolated with the saturated water content at the depth of 18 cm (i.e., bottom of the first layer), the measured water content at the depth of 33 cm (0.392 in 2007 and 0.384 in 2008) and 58 cm (0.414 in 2007 and 0.412 in 2008), and the saturated water content at the water table (0.483). Similarly, initial measured NH_4^+—N and NO_3^-—N concentration values of all soil layers were also given for initial N conditions. The initial urea concentrations for all soil profiles were zero. All simulations were conducted in daily time step from rice transplanting. The days were referred as days after transplanting (DAT).

For the HYDRUS-1D model simulation of soil water flow and N transport and transformation in experimental plots, the top boundary was set as an atmospheric boundary condition with surface layer to allow interactions between soil and atmosphere.

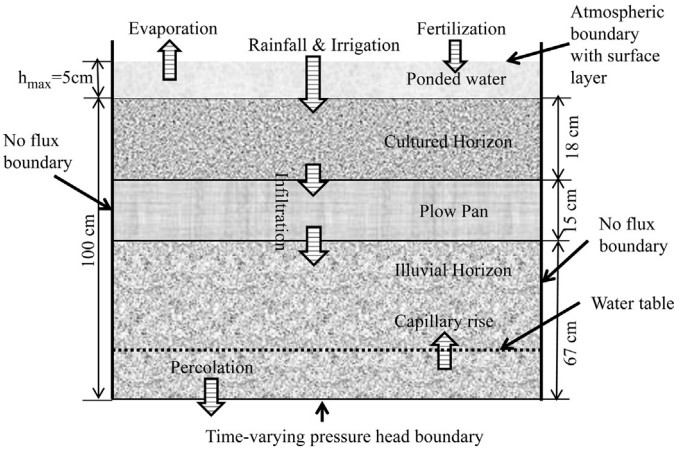

Fig. 2. Schematic representation of the modeling domain and its initial and boundary conditions.

These interactions including rainfall, irrigation, evaporation and fertilization were given in the time-variable boundary conditions by the measured data. The maximum ponded water depth was 5 cm as the irrigation schedule designed. Irrigation was regarded as rainfall ignoring spatial heterogeneity. With the atmospheric boundary condition, water evaporates from the soil surface at the potential evaporation E_p, as the pressure head at the surface were always higher than the assumed threshold value, h_{crit} (−15,000 cm). The Cauchy type (third-type) boundary conditions were used to represent the urea fertilization to the ponded water. The bottom boundary condition was the measured daily piezometric head at the bottom (Fig. 3). Both left and right sides of the plots were assigned with the no flux boundary condition. The Dirichlet type (first-type) boundary condition was employed for the bottom boundary condition given by the N concentrations in the bottom for N transport and transformation simulation.

2.2.5. Model parameters

For obtaining the soil hydraulic parameters to drive the HYDRUS-1D simulation, undisturbed soil samples (100 cm^3) were collected from different soil layers of three randomly selected paddy plots after the rice harvesting in 2011 to carry out supplementary measurement of soil hydraulic properties. Samples were firstly used to measure the saturated hydraulic conductivity by constant head method. The soil water retention curve, $\theta(h)$ (van Genuchten, 1980), was determined in laboratory using with the Hyprop System based on the simplified evaporation method (Peters and Durner, 2008). Because there was heterogeneity and preferential flow in paddy fields, especially paddy plots under AWD irrigation (Garg et al., 2009; Sander and Gerke, 2009), the point measured soil hydraulic properties cannot fully represent the field soil properties. Therefore, the measured saturated hydraulic

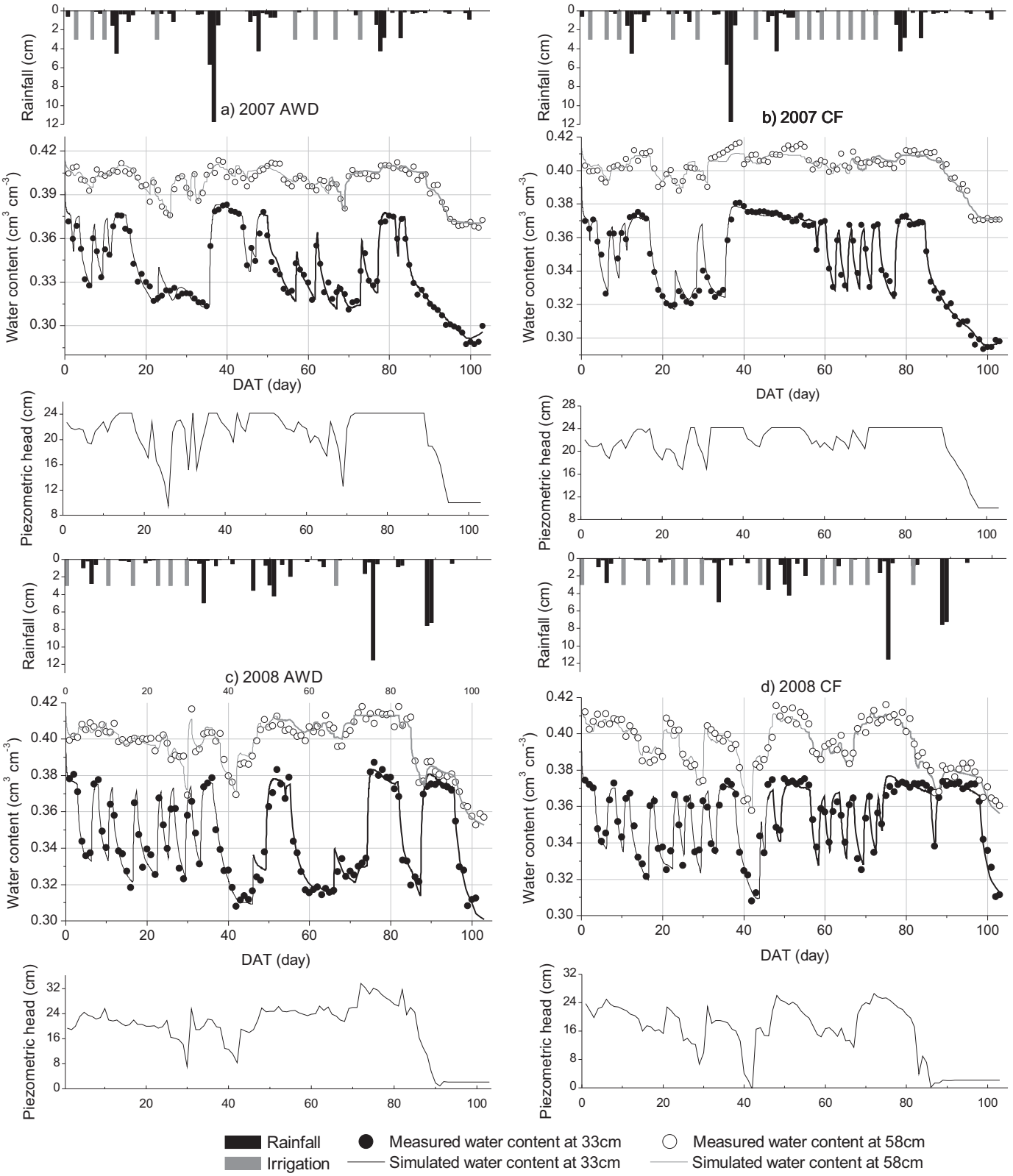

Fig. 3. Measured (TDR) and simulated (HYDRUS-1D) volumetric water contents varying with the rainfall and irrigation, at soil depth of 33 and 58 cm in paddy plots under AWD and CF irrigation during the rice growing season of 2007 and 2008. The piezometric head of the domain bottom is also shown.

conductivity (K_s) of plow pan was calibrated for improving the simulation of water flow as Tan et al. (2014) previously did. The measured and calibrated soil hydraulic parameters are shown in Table 2. During the simulation, identical averaged soil hydraulic parameters were used for all experimental plots under AWD or CF irrigation, respectively, since the area of the fields is small and the spatial variability of soil hydraulic properties on water flow and N transport can be neglected.

NH_4^+—N was assumed to be adsorbed by the paddy soil to the solid phase with the distribution coefficient of 3.5 $cm^3\ g^{-1}$

(Dash et al., 2014; Hanson et al., 2006; Ling and El-Kadi, 1998; Lotse et al., 1992; Ramos et al., 2011). The N transport parameter, longitudinal dispersivity (D_L), as well as N transformation parameters including $\mu'_{w,1}$ (hydrolysis), $\mu'_{w,2}$ and $\mu'_{s,2}$ (nitrification in the liquid and solid phases), $\mu_{w,2}$ and $\mu_{s,2}$ (volatilization), $\gamma_{w,2}$ and $\gamma_{s,2}$ (mineralization and bio-fixation) and $\mu_{w,3}$ and $\mu_{s,3}$ (denitrification) cannot be easily measured in laboratory or on field. These parameters were calibrated from comparing measured and simulated NH_4^+—N and NO_3^-—N concentrations in soil water using the published range of N transformation constants presented by Chowdary et al. (2004) and Hanson et al. (2006), with the objective of minimizing the differences of measured and simulated NH_4^+—N and NO_3^-—N concentrations. The calibrated N transport and transformation parameters using collected data of plots under all N treatments were show in Table 3.

2.2.6. Model simulations and performance

Field simulations using HYDRUS-1D began on the day of rice transplanting (June 6 in 2007, and June 2 in 2008), at the beginning of rice growing season, and lasted 103 days to rice harvesting. Both water and N treatments were assumed to be factors that induced the difference of water and N regime between paddy plots. As there were no significant variations of water and N regime between paddy plots with the same water and N treatments (Tan et al., 2013), measured data of four replicates were averaged to decrease the number of simulation. Therefore, twelve data sets (2 water × 3 N × 2 years) for water and N treatment combinations were derived. Water and N regime of these six composite experimental paddy plots within two rice growth seasons were simulated accordingly.

Several calibration and validation exercises for each paddy plots were carried out to determine the parameters including K_s, D_L, $\mu'_{w,1}$, $\mu'_{w,2}$, $\mu'_{s,2}$, $\mu_{w,2}$, $\mu_{s,2}$, $\gamma_{w,2}$, $\gamma_{s,2}$, $\mu_{w,3}$ and $\mu_{s,3}$ that were too difficult to be measured, and establish the model predictability of this set of parameters. Since it was extremely hard to have a good performance of the N simulation with the same N transformation parameters for all N treatments, we used three groups of transformation parameters for the low, medium and high N treatments (Table 3), respectively. Several calibration and validation exercises were carried out to establish the predictability of soil saturated hydraulic conductivities and N transport and transformation parameters for each plot. For example, soil saturated hydraulic conductivities calibrated with the measured soil water content in 2007 (2008) were used as input to predict the soil water content in 2008 (2007).

In addition to visual checks, field measured values of soil water contents and N concentrations were compared with the values from HYDRUS-1D simulation using the root mean square error (RMSE) and Nash–Sutcliffe modeling efficiency (NSE) given by:

(i) Root mean square error (RMSE):

$$\mathrm{RMSE} = \sqrt{\frac{1}{n-p}\sum_{i=1}^{n}(P_i - O_i)^2} \tag{14}$$

(ii) Nash–Sutcliffe modeling efficiency (NSE) (Nash and Sutcliffe, 1970):

$$\mathrm{NSE} = 1 - \frac{\sum_{i=1}^{n}(O_i - P_i)^2}{\sum_{i=1}^{n}(O_i - O)^2} \tag{15}$$

where P_i is the predicted value corresponding to the observed value O_i, and n is the number of data pairs and p is the number of parameters estimated during optimization. O is the observed mean value.

Table 3
N transport and transformation parameters for experimental soil profile derived from model calibration.

Soil layer	D_L (cm)	$\mu'_{w,1}$ (day^{-1})	K_d (cm^3 g^{-1})	$\mu_{w,2}$ (day^{-1})	$\mu'_{w,2}$ (day^{-1})	$\mu'_{s,2}$ (day^{-1})	$\mu_{w,3}$ (day^{-1})	$\mu_{s,3}$ (day^{-1})	$\gamma_{w,2}$ (g cm^{-3} day^{-1})	$\gamma_{s,2}$ (g cm^{-3} day^{-1})
Range	5	0.3–0.8	3–4	0.02–0.07	0.02–0.72	0.02–0.72	0.01–0.24	0.01–0.24	0.001–0.04	0.001–0.04
N fertilization rate = 0 kg ha^{-1}										
Cultivated horizon (0–18 cm)	7.0	–	3.5	0.02	0.085	0.085	0.06	0.06	0.20	0.20
Plow pan (18–33 cm)	3.2	–	3.5	0	0.055	0.055	0.15	0.15	0.10	0.10
Illuvial horizon (33–100 cm)	6.4	–	3.5	0	0.03	0.03	0.1	0.1	0	0
N fertilization rate = 135 kg ha^{-1}										
Cultivated horizon (0–18 cm)	7.0	0.65	3.5	0.02	0.10	0.10	0.1	0.1	0.08	0.08
Plow pan (18–33 cm)	3.2	0.65	3.5	0	0.075	0.075	0.25	0.25	0.06	0.06
Illuvial horizon (33–100 cm)	6.4	0.65	3.5	0	0.03	0.03	0.2	0.2	0	0
N fertilization rate = 180 kg ha^{-1}										
Cultivated horizon (0–18 cm)	7.0	0.7	3.5	0.03	0.11	0.11	0.1	0.1	0.04	0.04
Plow pan (18–33 cm)	3.2	0.7	3.5	0	0.075	0.075	0.25	0.25	0.04	0.04
Illuvial horizon (33–100 cm)	6.4	0.7	3.5	0	0.03	0.03	0.2	0.2	0	0

Note: The range of parameters were referred to the publications, such as Antonopoulos (2010), Chowdary et al. (2004), Dash et al. (2014), Hanson et al. (2006), Ling and El-Kadi (1998) and Lotse et al. (1992); D_L, longitudinal dispersivity; K_d, ammonium distribution coefficient; $\mu'_{w,1}$, first-order rate constant of hydrolysis; $\mu_{w,2}$, first-order decay coefficients of volatilization; $\mu'_{w,2}$ and $\mu'_{s,2}$, first-order rate constant of nitrification in the liquid and solid phases, respectively; $\mu_{w,3}$ and $\mu_{s,3}$, first-order decay rate constant of denitrification in the liquid and solid phases, respectively; $\gamma_{w,2}$, zero-order mineralization and bio-fixation rate constant.

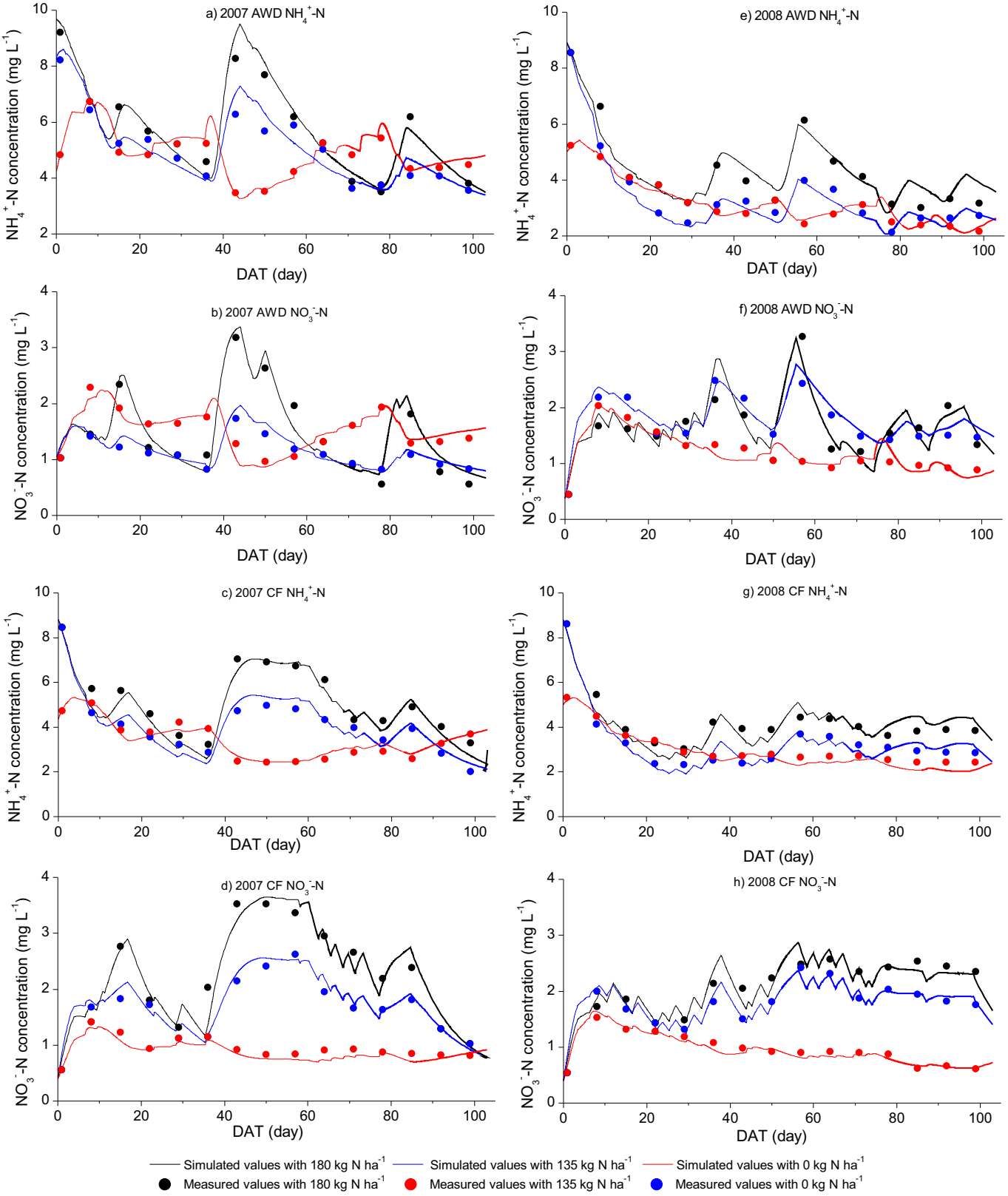

Fig. 4. Comparison of simulated and measured NH_4^+—N and NO_3^-—N concentrations at soil depth of 33 cm in paddy plots under AWD and CF irrigation during the rice growing season of 2007 and 2008.

The closer the root mean square error (RMSE) is to 0, the more accurate the model is. Modeling efficiencies (NSE) can range from $-\infty$ to 1. Generally, the closer the model efficiency is to 1, the more accurate the model is.

3. Results and discussion

Although measured and simulated soil water content data at depth of 33 and 58 cm were compared for all twelve experimental

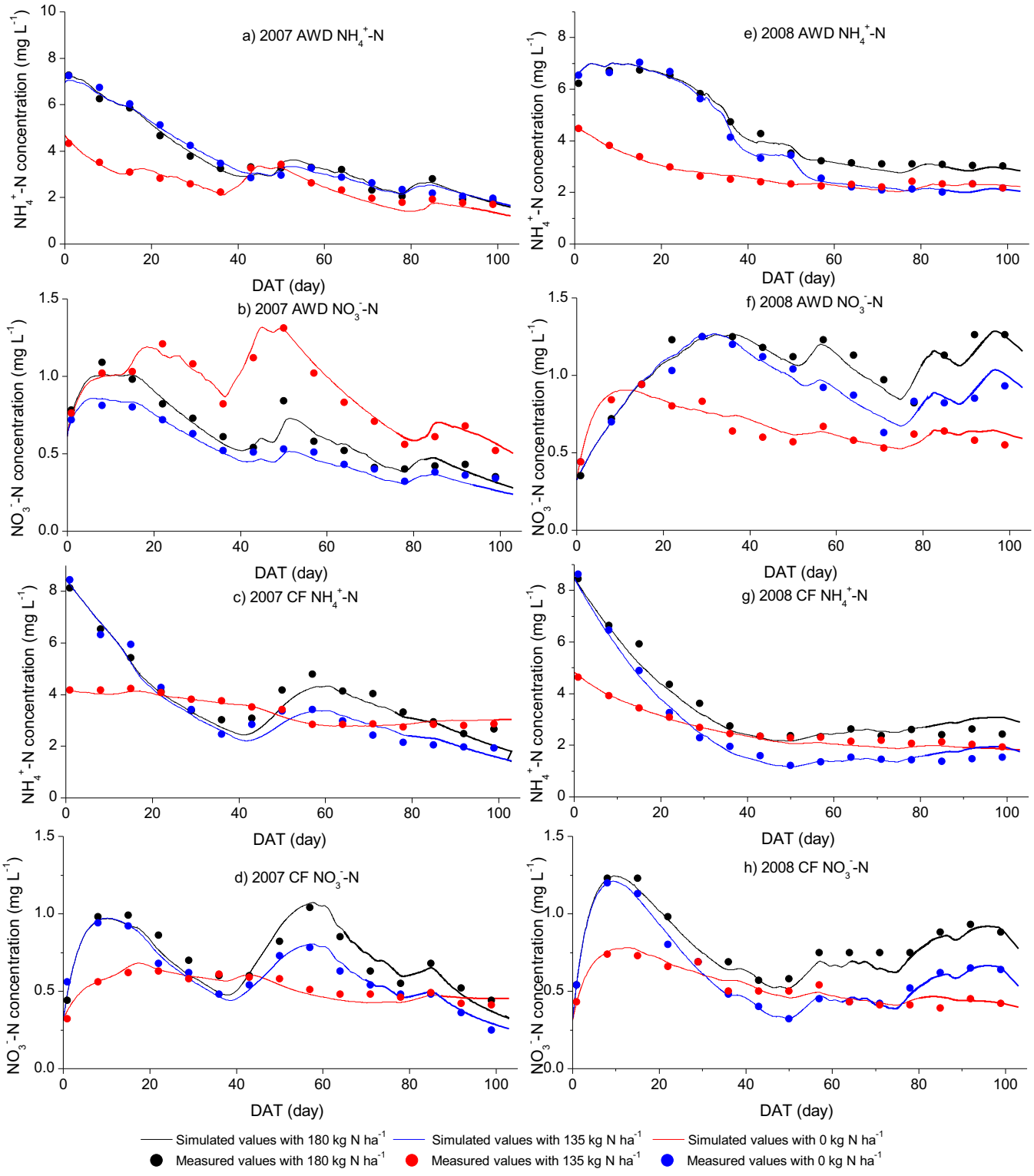

Fig. 5. Comparison of simulated and measured NH_4^+—N and NO_3^-—N concentrations at soil depth of 58 cm in paddy plots under AWD and CF irrigation during the rice growing season of 2007 and 2008.

paddy plots, only results for the AH and CH treatments at depth of 33 and 58 cm are presented graphically in Fig. 3, in order to limit the number of figures and maintain consistency. The measured and simulated N regime at depth of 33 (Fig. 4) and 58 (Fig. 5) cm are shown in all six paddy plots. The statistical analysis presented in Table 4 involves model performance results obtained for all twelve composite treatments.

3.1. Soil water content in soil profile

Fig. 3 shows the comparison of water contents measured with TDRs and water contents derived from HYDRUS-1D simulations in AWD and CF paddy plots with N input of 180 kg ha^{-1}. Some minor differences found between measured and simulated water contents can be explained by the fact that the divisions of soil

Table 4
Comparison between measured and simulated soil water content, NH_4^+—N and NO_3^-—N obtained for the soil depth of 33 and 58 cm averaged of the year 2007 and 2008.

Water and nitrogen treatments[a]		RMSE[b]			NSE[b]		
	Water content (cm^{-3} cm^{-3})	NH_4^+—N (mg L^{-1})	NO_3^-—N (mg L^{-1})	Water content	NH_4^+—N	NO_3^-—N	
AL	2007	0.02	0.28	0.07	0.97	0.81	0.84
	2008	0.01	0.32	0.06	0.96	0.84	0.84
CL	2007	0.02	0.25	0.05	0.96	0.86	0.85
	2008	0.02	0.30	0.08	0.95	0.83	0.79
AM	2007	0.01	0.27	0.08	0.98	0.85	0.82
	2008	0.02	0.26	0.04	0.97	0.84	0.87
CM	2007	0.02	0.19	0.04	0.95	0.83	0.87
	2008	0.02	0.22	0.05	0.95	0.85	0.83
AH	2007	0.01	0.21	0.06	0.98	0.87	0.86
	2008	0.01	0.17	0.06	0.97	0.85	0.91
CH	2007	0.02	0.16	0.05	0.96	0.87	0.87
	2008	0.01	0.23	0.04	0.97	0.81	0.88

[a] A and C are the irrigation techniques of AWD and CF, respectively; L, M and H is the nitrogen fertilization amount rate of 0, 135 and 180 kg ha^{-1}, respectively.
[b] RMSE, Root mean square error; NSE, Nash–Sutcliffe modeling efficiency.

layers were not very accurate. Usually the soil texture and hydraulic parameters were changing gradually in the soil profile, but we just used significantly different parameters for two adjacent soil layers. Increasing the soil layers with gradually varying hydraulic parameters will improve the simulation of the water regime of soil profile. However, the simulated water contents, overall, agree well with measured water contents as the statistical results for model performance were very high (Table 3). The modeling water regime of paddy plots was reasonable to be used for N regime modeling and analysis.

There were no significant variations of water regime between paddy plots under different N fertilization as measured (Tan et al., 2013) and simulated. The irrigation techniques, i.e., AWD and CF, were the main factors resulting in different field soil water regime. The minor differences (not shown) between the plots with different N treatments but the same irrigation technique were in the vertical soil water content distribution, because the different partitions of the evapotranspiration to evaporation and transpiration (rice root water uptake) in case that the rooting depth of AWD plots was higher than that of CF plots. However, for the water balance calculation, this difference disappeared as we used the same evapotranspiration value for the AWD or CF plots with different N treatments.

Before the rice growth stage of late tillering, the water contents in AWD and CF plots were almost the same because of the same irrigation practice according to the irrigation schedule. However, after late tillering, the differences of water contents between paddy plots under AWD and CF irrigation were significant both in 2007 and 2008 due to the different irrigation practice. Soils both at depth of 33 and 58 cm were seldom saturated, even though there were many field ponded days when soils at depth of 0–18 cm were mostly saturated both in AWD and CF plots. It highlights the importance of plow pan for the decrease of the infiltration and the formation of ponded water. Note that the soil water contents at depth of 18 cm, which are not shown in the figure, varied greatly with the irrigation and rainfall during the rice growing season. The pressure head of the soil at depth of 18 cm of AWD plots even amounted to −200 cm at DAT = 35 in 2007 and DAT = 36 in 2008, which was the driest water regime during the experiments. The rice water uptake was not reduced by the water stress since the threshold of pressured head was set to −300 cm. That is why the rice water uptake was the potential water uptake for all paddy plots (Table 5). Therefore, the grain yield of rice remained unaffected in paddy plots irrigated according to the schedule of both AWD and CF (Tan et al., 2013).

3.2. Water balances

Considering 100 cm deep soil profile as a single system, the water balance components during the rice growing season in 2007 and 2008 are shown in Fig. 6. There was a large amount of water lost by percolation that amounted to 55.6 and 64.4% in 2007, and 73.7 and 73.6% in 2008 of water input (rainfall and irrigation), in AWD and CF plots, respectively. It means that the percolation was decreased by 27.8 and 19.0% in 2007 and 2008, respectively, benefiting from the practice of AWD irrigation, compared to CF irrigation. Since the evapotranspiration was assumed to be the same in plots under AWD and CF irrigation, AWD irrigation decreased 38.5 and 50.0% of irrigation water on average in 2007 and 2008, respectively, compared to CF irrigation. Because plots were ponded at the start of the rice growing seasons and naturally drained at the end, soil water was also depleted for rice growth (Fig. 6). The amount of evapotranspiration (41.2 cm) in 2007 was 54.2 and 45.2% of the applied water, and 33.6 cm water for evaporation in 2008 only occupied 44.0 and 35.6% of the applied water in AWD and CF plots, respectively. These rates indicate that the AWD irrigation enhanced the water use efficiency compared to CF irrigation.

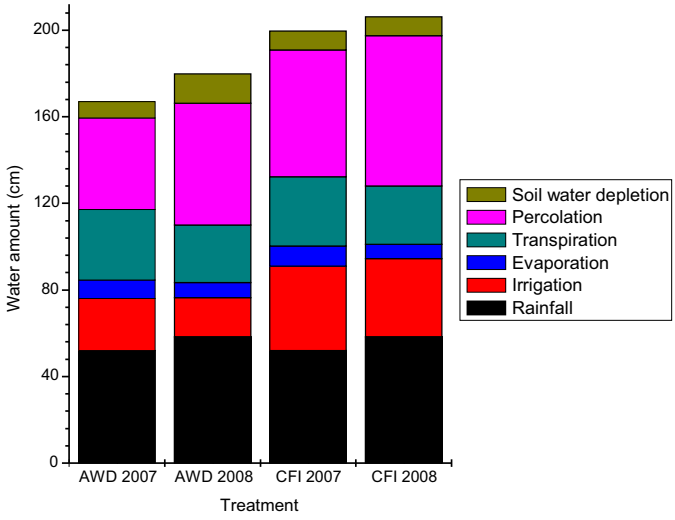

Fig. 6. Water balance in paddy plots with AWD and CF irrigation.

3.3. Nitrogen concentrations

It was difficult to calibrate the model to minimize the differences between measured and simulated N concentrations at all two measured depths in both AWD and CF paddy plots with three N treatments with the same soil transformation parameters. This was due to the several factors that influence the N transformation rate constants, such as N concentrations, soil pH, soil temperature,

Table 5
Simulated N balance in experimental plots under AWD and CF irrigation with three N treatments.

Water and nitrogen treatments[a]	AL		CL		AM		CM		AH		CH	
	2007	2008	2007	2008	2007	2008	2007	2008	2007	2008	2007	2008
NH_4^+—N												
Fertilization (kg ha^{-1})	0.0	0.0	0.0	0.0	135.0	135.0	135.0	135.0	180.0	180.0	180.0	180.0
Rainfall and irrigation (kg ha^{-1})	1.2	1.4	1.3	1.5	1.3	1.4	1.6	1.7	1.4	2.1	1.8	2.3
Mineralization and bio-fixation (kg ha^{-1})	100.5	98.3	92.4	93.7	65.4	55.3	60.4	52.8	44.3	38.7	37.5	35.6
Volatilization (kg ha^{-1})	10.2	5.3	8.4	4.7	27.8	24.6	23.3	20.9	30.6	28.4	28.9	27.7
Nitrification (kg ha^{-1})	42.6	40.1	39.4	37.9	57.8	55.3	52.8	51.4	64.3	58.4	60.5	55.9
Rice uptake (kg ha^{-1})	62.3	57.2	64.4	62.9	83.5	78.6	87.4	71.4	92.8	87.5	96.2	94.7
Leaching (kg ha^{-1})	7.8	4.3	8.8	4.5	14.1	8.5	14.8	10.6	16.8	13.5	18.2	15.3
Soil NH_4^+—N accumulation (kg ha^{-1})	−21.2	−7.2	−27.2	−14.8	18.5	24.7	18.7	35.2	21.2	33.1	15.5	24.3
NO_3^-—N												
Rainfall and irrigation [b] (kg ha^{-1})	4.0	4.6	4.4	5.1	4.4	4.6	5.5	5.5	4.7	4.8	6.0	6.2
Rice uptake (kg ha^{-1})	16.9	15.3	18.8	17.2	24.2	22.6	26.8	24.9	28.3	27.0	30.2	28.7
Denitrification (kg ha^{-1})	22.4	20.5	18.7	21.4	32.5	29.7	28.5	26.7	33.6	30.8	31.5	29.6
Leaching (kg ha^{-1})	2.1	0.9	2.3	0.9	1.9	0.8	2.1	0.8	1.9	0.6	2.3	0.7
Soil NO_3^-—N accumulation (kg ha^{-1})	5.1	8.0	4.0	3.6	3.5	6.8	0.9	4.5	5.3	4.8	2.5	3.1
Total N leaching (kg ha^{-1})	9.9	5.2	11.1	5.4	16.1	9.3	16.9	11.4	18.7	14.1	20.5	16.0
N input (kg ha^{-1})	100.5	98.3	92.4	93.7	200.4	190.3	195.4	187.8	224.3	218.7	217.6	215.6
Total N uptake (kg ha^{-1})	79.2	72.5	83.2	80.1	107.7	101.2	114.2	96.3	121.1	114.5	126.4	123.4

[a] A and C are the irrigation techniques of AWD and CF, respectively; L, M and H is the nitrogen fertilization amount rate of 0, 135 and 180 kg ha^{-1}, respectively.

aeration, C/N ratio, cation exchange capacity, etc. The effects of these factors on the changes of rate constants were summarized by Chowdary et al. (2004). We cannot consider all these factors in simulation. The N concentrations were varied greatly in paddy plots under different N treatments, so the N transformation parameters were calibrated for each N treatment. The three groups of N transformation parameters obtained from calibration are shown in Table 3. The model performance statistics of N simulations shown in Table 4 indicates good simulation results, as the RMSE of NH_4^+—N and NO_3^-—N concentration for all treatments ranged 0.16–0.32 and 0.04–0.08, respectively. The model efficiency NSE ranged from 0.79 to 0.91, which implies a good agreement between observed and simulated values.

Our modeling approach, to some extent, suggests the inappropriateness of using the same N transformation parameters for N regime simulation in plots with different N treatments. However, the same N transformation parameters were usually applied to model the potential N regime and balance under different N fertilization scenarios, such as Dash et al. (2014). The N transformation process is extremely complicated in paddy fields, using the zero- and/or first-order decay reaction cannot fully describe this time-varying process. Moreover, the rate constants are varying with many factors (Chowdary et al., 2004), and the carbon cycle in the paddy fields of great significance to the N transformation. Therefore, many models coupling the water, carbon and N processes were developed to simulate the N regime in paddy fields, e.g., Berlin et al. (2014), Oulehle et al. (2012) and Katayanagi et al. (2013). The N concentration is the most familiar one that is significantly different in paddy plots with different N fertilizations, so more effects should be taken to examine the model predictability under different specific conditions. Coupling biological process to the N transformation may further improve the model performance.

Figs. 4 and 5 show the comparison of simulated and measured NH_4^+—N and NO_3^-—N concentrations in plots at soil depth of 33 and 58 cm, respectively. Their fluctuations were described in detail in our previous paper (Tan et al., 2013). However, more subtle N concentration variations with time were observed by model simulation, which would increase the accuracy of calculating the N balances, compared to just using simple linear interpolation data from limited measured N concentrations and water fluxes. Since soil water samplings and N concentration measurements were only taken weekly basis, some extremely large or small concentration values happened in plots were hard to be observed with this low sampling frequency. This was especially obvious in plots under AWD where soil water content varied a lot and N may be diluted or concentrated. Since there was deep ponded water in plots when urea applied, the concentration varied with urea application was not much evident. However, the dynamics of N flux were concurrent with the urea application as simulated.

3.4. Nitrogen balances

The cumulative amount of each N balance component of plots under all treatments during the whole rice growing season was obtained from model simulation and shown in Table 5. The HYDRUS-1D was operated for the rice field and the depth of NH_4^+—N and NO_3^-—N load converged at 100 cm depth below ground surface and the simulated amount was, on average, 7.9, 13.4, and 17.3 kg ha^{-1} for the N fertilization of 0, 135 and 180 kg ha^{-1}, respectively. Note that the percentages of N leaching losses to N fertilizer applied ranges from 6.9 to 12.5%, which is much lower than that (55.6–73.7%) of the percolation water to water input. It is very true that the N leaching losses are percolation driven in the field. However, in the soil profile of our paddy plots, the N content distribution varied significantly from top to bottom. The N content in upper (0–33 cm) soil water is, on average, at least less than 1/5 of that in lower (34–100 cm) soil water. Since the organic matter contents and biological activities in the upper soil were greatly higher than that in the lower soil (Table 1), the N reaction parameters in the upper soil were greatly higher than that in the lower soil (Table 3). Moreover, the compaction of plow pan and its low hydraulic conductivity decreased the water and solution movement in the whole profile of paddy fields (Tournebize et al., 2006; Patil et al., 2011). Therefore, the soil water and N was usually retained in the upper soil to have enough hydraulic retention time to be transformed and/or absorbed by rice, which strengthened the volatilization and denitrification process that produced N-gases and emitted to the atmosphere, and the immobilization process that made the NH_4^+—N be absorbed by soil particles. These characteristics resulted in the extremely low N content in the leaching water and relatively low N leaching losses. The N leaching losses in two years, 12.8 kg ha^{-1} on average were both significantly lower than that the reported value (120 kg ha^{-1}) that Chowdary et al. (2004) and Antonopoulos (2010) obtained, and 28.5 kg ha^{-1} simulated by Dash et al. (2014). Their high N leaching losses were resulted from the high hydraulic conductivity of the plow pan soil.

The average values of total N leaching losses in the AWD and CF paddy plots were 12.2 and 13.5 kg ha^{-1}, which are in agreement with measured N leaching losses (Tan et al., 2013) in which NH_4^+—N leaching losses in plots under AWD were lower than that under CF plots. Total N leaching losses were decreased 5.0–11.2% in 2007 and 3.0–23.5% in 2008 by AWD irrigation, compared to CF irrigation. However, simulated NH_4^+—N leaching losses in this study were slightly different from that the measured ones. Average NO_3^-—N leaching losses simulated in plots under AWD (1.4 kg ha^{-1}) were slightly lower than that under CF (1.5 kg ha^{-1}), while average NO_3^-—N leaching losses measured in plots under AWD (1.6 kg ha^{-1}) were higher than that under CF (1.3 kg ha^{-1}). As the NO_3^-—N leaching losses were only 4.7–27.3% of NH_4^+—N leaching losses, these slight variations in simulated and measured NO_3^-—N leaching losses values were not of importance to assess the N leaching losses in our experiment plots.

The average values of N uptake in the AWD and CF paddy plots were 99.4 and 103.9 kg ha^{-1}, which is consistent to the non-significant effect of AWD irrigation on the rice yield as the field experiments showed (Tan et al., 2013), compared to CF irrigation. Except in the plots with medium N application in 2008, where the rice uptake of NH_4^+—N in the AWD plot was higher (10.1%) than that in the CF plot, all plots with AWD irrigation exhibiting a slightly lower (4.2–9.5%) N uptake than that with CF irrigation (Table 5). However, Dong et al. (2012) experimented the N balances using ^{15}N-labeled method and found that AWD increased the rice N uptake by 13.6% on average, compared to CF. Therefore, the effect of AWD on the rice N uptake should be further examined on the specific field conditions such as soil properties and N fertilization.

Mineralization and bio-fixation contributed 41.5 and 36.6 kg ha^{-1} N for paddy plots under AH and CH in the two rice growing season, which was significantly lower than that under AL (99.4 kg ha^{-1}), CL (93.1 kg ha^{-1}), AM (60.4 kg ha^{-1}) and CM (56.6 kg ha^{-1}) treatments. Dash et al. (2014) simulated that the mineralization and bio-fixation N amounted to 75.6 kg ha^{-1} in paddy fields with N application of 120 kg ha^{-1}, which is similar to our results on plots with N application of 135 kg ha^{-1}. Gaydon et al. (2012) summarized that estimates of mineralized and fixed N vary from a few to 80 kg ha^{-1}. Plots with no N fertilization had high mineralization and fixed N and resulted in the high depletion of the soil N storage (Table 5). The average mineralization and bio-fixation was 9.15 mg kg^{-1} soil which was significantly lower than that reported values of continuously flooded paddy soil (24.1 mg kg^{-1} soil) (Antonopoulos, 2010), which was fertilized with lower N and large leaching water took much oxygen for N mineralization. The bio-fixation was more intense in fields where the soil was waterlogged throughout the year than in nearby fields with intermittent waterlogging (Okuda and Yamaguchi, 1952), thus, AWD fields usually have lower bio-fixation rate than CF fields. However, N-mineralization rates were significantly higher in the plots under AWD than that under CF, because of the alternate aerobic and anaerobic environment (Dong et al., 2012). Therefore, the effect of AWD on the mineralization and bio-fixation were difficult to be detected by lumped mineralization and bio-fixation processes as this study did. Since our objective was to simulate field experiments in a relatively simple way by fully using the HYDRUS-1D model, lumping mineralization and bio-fixation together seemed to be sufficient to describe N regime in these composite plots.

The nitrification amount in plots under AWD irrigation was higher (6.3–9.4% in 2007 and 4.5–7.6% in 2008) than that under CF irrigation, on average of N treatments, which is as expected since the aerobic environment sometimes happened in AWD plots was favorable to the nitrification. Thus, the NH_4^+—N concentrations in plots under CF were generally larger than that under AWD as more NH_4^+—N was nitrified in AWD plots (Figs. 4 and 5).

The major pathway of nonproductive N losses in all plots was denitrification that accounted for on average 19.6% of urea fertilization, although denitrified N was not all from the urea fertilization. The amount of NO_3^-—N denitrified in AWD plots was 6.7–19.8% in 2007 and 4.1–11.2% in 2008 higher than that in CF plots, except that of the AWD plot in 2008 was 4.2% lower than that of the CF plot. This was caused by the more frequent wetting and drying cycles, because that the increased NO_3^-—N from nitrification of NH_4^+—N in the drying phase with aerobic environment can be easily denitrified to N_2 or N_2O in the wetting phase with anaerobic environment (Buresh et al., 2008; Dong et al., 2012). As the soil water regime in AWD plots at our experiment was relatively saturated than that at experiments conducted by Dong et al. (2012), the intensification of the processes of nitrification–denitrification in our experiments was not as evident as theirs. Dong et al. (2012) found that N_2 emission from nitrification–denitrification for the AWD treatment was about 6 times higher than for the CF treatment. The N denification increased with the N application. The denitrified N range during the rice growing season, 18.7–33.6 kg ha^{-1}, was slightly lower than simulated value 38–40 kg ha^{-1} (Antonopoulos, 2010) for plots with high percolation, hihger than simulated value 18.9 kg ha^{-1} (Dash et al., 2014) for plot with 120 kg ha^{-1} N application, and similar to the measured value 33 kg ha^{-1} (Pathak et al., 2004) and simulated value 30.4 kg ha^{-1} (Ebrayi et al., 2007).

N losses by volatilization in plots under AWD were also significantly (6.0–22.0% in 2007 and 2.5–11.7% in 2008) higher than that under CF. The variations of volatilization between two rice growing seasons was also, as nitrification, caused by the relatively wet soil water regime and low NH_4^+—N concentration in 2008 due to the larger rainfall, compared to in 2007 (Fig. 3). The average N volatilization losses were 7.1, 24.2 and 28.9 kg ha^{-1} for plots with 0, 135, and 180 kg ha^{-1} N application, which is consistent to the reported value 20–30 kg ha^{-1} (Ebrayi et al., 2007; Dash et al., 2014). Note that limited by the availability of HYDRUS-1D for describe the N transformation processes with sequential first-order decay chains (Ramos et al., 2011), processes to decrease the NH_4^+—N other than volatilization and nitrification were not considered, such as immobilization process in which soil organisms of lowland rice assimilate inorganic NH_4^+—N compounds and transform them into organic N constituents of their cells, tissues and soil mass. Therefore, the simulated volatilization losses may include the immobilized NH_4^+—N that had been mineralized in plots but volatilized to the atmosphere, as mineralization and immobilization are N-transformation processes which occur simultaneously in flooded soils.

The increasing effect of AWD irrigation on nitrification and N losses through denitrification, volatilization reflects the intensified nitrification–denitrification processes that were caused by the relatively high NH_4^+—N concentration, and alternate aerobic and anaerobic environment in AWD paddy fields. The increased nitrate, which was formed from nitrification of ammonium in drying (aerobic) phase, can be easily denitrified to N_2 or N_2O in the wetting (anaerobic) phase. Therefore, the practice of AWD irrigation should consider its side effects on increasing N emissions from paddy fields that may also decrease the N use efficiency. The N balances (Table 5) show that soil profiles of plots with medium and high N application was accumulated with NH_4^+—N after rice harvest, while plots with no N application depleted soil N storage. NH_4^+—N reserved in soil profile of the AWD plots with high (medium) N application was higher (lower) than the CF plots because of different transformation rates and field N regime. Further long-term N balance simulation should be conducted to assess the soil N storage variation for sustainable rice production, as this study did not investigate the N source of mineralization and the amount of rice straw returned to fields after rice harvesting.

4. Conclusions

HYDRUS-1D model was used to describe the N transport and transformations in lowland paddy fields under AWD and CF irrigation. Because of the low hydraulic conductivity of plow pan in the middle of paddy soil profile, the surface ponded water can slowly infiltrate to the deep soil and then be recharged by rainfall and irrigation. These dynamic boundary conditions in paddy fields both under AWD and CF irrigation were appropriately handled by HYDRUS-1D. Although the HYDRUS-1D model cannot fully describe N transformation processes with sequential first-order decay chains, the field N regime analysis and balance estimates can be carried out by lumping some similar N processes for HYDRUS-1D model simulation. The availability of describing soil water content dependent N transformation parameters also makes the HYDRUS-1D model to be useful for comparing the soil water and N regime in paddy fields under AWD and CF irrigation.

Simulation results provide detailed soil water and N regime, as well as bottom boundary flux for percolation and N leaching estimation. Generally, there were great variations of N fate between paddy fields under AWD and CF irrigation. The processes of nitrification–denitrification, mineralization and voltalization were intensified by AWD, compared to CF, which may increase the greenhouse gas (N_2O and NH_4) emissions. The success of the AWD practice for rice production should take the environmental effects of AWD into consideration. Although the influence of parameter uncertainties on the simulation results should be considered for future works, modeling by HYDRUS-1D is a useful system approach that covers all processes related to water and N management for supporting the strategic and tactical decision process in sustainable rice production.

Acknowledgements

This work was financially supported by the National Key Technologies R&D Program of China during the 12th Five-year-Plan Period (no. 2012BAD08B05) and the National Natural Science Foundation of China (nos. 51379150 and 51439006).

References

Ajdary, K., Singh, D.K., Singh, A.K., Khanna, M., 2007. Modelling of nitrogen leaching from experimental onion field under drip fertigation. Agric. Water Manage. 89 (1–2), 15–28.

Allen, R.G., Pereira, L.S., Raes, D., Smith, M., 1998. Crop evapotranspiration—guidelines for computing crop water requirements. In: FAO Irrigation and Drainage. Food and Agriculture Organization (FAO) of the United Nations, Rome, Italy, pp. 56 (Paper 56).

Antonopoulos, V.Z., 2010. Modelling of water and nitrogen balances in the ponded water and soil profile of rice fields in Northern Greece. Agric. Water Manage. 98 (2), 321–330.

Belder, P., 2004. Effect of water-saving irrigation on rice yield and water use in typical lowland conditions in Asia. Agric. Water Manage. 65 (3), 193–210.

Belder, P., Spiertz, J., Bouman, B., Lu, G., Tuong, T., 2005. Nitrogen economy and water productivity of lowland rice under water-saving irrigation. Field Crop Res. 93 (2–3), 169–185.

Berlin, M., Suresh Kumar, G., Nambi, I.M., 2014. Numerical modelling on transport of nitrogen from wastewater and fertilizer applied on paddy fields. Ecol. Model. 278, 85–99.

Bouman, B., Humphreys, E., Tuong, T., Barker, R., 2007. Rice and water. Adv. Agron. 92, 187–237.

Bouman, B.A.M., Kropff, M.J., Tuong, T.P., Wopereis, M.C.S., tenBerge, H.F.M., vanLaar, H.H., 2001. ORYZA2000: Modelling Lowland Rice. International Rice Research Institute, Wageningen University and Research Centre, Los Banos, Philippines, Wageningen, Netherlands, pp. 235.

Buresh, R.J., Reddy, L.R., van Kessel, C., 2008. Nitrogen transformations in submerged soils. In: Schepers, J.S., Raun, W.R. (Eds.), Nitrogen in Agricultural Systems. American Society of Agronomy, Madison, WI, pp. 401–436.

Cabangon, R.J., Castillo, E.G., Tuong, T.P., 2011. Chlorophyll meter-based nitrogen management of rice grown under alternate wetting and drying irrigation. Field Crop Res. 121 (1), 136–146.

Cabangon, R.J., Tuong, T.P., Castillo, E.G., Bao, L.X., Lu, G., Wang, G., Cui, Y., Bouman, B.A.M., Li, Y., Chen, C., Wang, J., 2004. Effect of irrigation method and N-fertilizer management on rice yield, water productivity and nutrient-use efficiencies in typical lowland rice conditions in China. Paddy Water Environ. 2 (4), 195–206.

Chowdary, V., Rao, N.H., Sarma, P.B.S., 2004. A coupled soil water and nitrogen balance model for flooded rice fields in India. Agric. Ecosyst. Environ. 103 (3), 425–441.

Crevoisier, D., Popova, Z., Mailhol, J.C., Ruelle, P., 2008. Assessment and simulation of water and nitrogen transfer under furrow irrigation. Agric. Water Manage. 95 (4), 354–366.

Dash, C.J., Sarangi, A., Singh, D.K., Singh, A.K., Adhikary, P.P., 2014. Prediction of root zone water and nitrogen balance in an irrigated rice field using a simulation model. Paddy Water Environ., http://dx.doi.org/10.1007/s10333-014-0439-x.

Dong, N.M., Brandt, K.K., Sorensen, J., Hung, N.N., Hach, C.V., Tan, P.S., Dalsgaard, T., 2012. Effects of alternating wetting and drying versus continuous flooding on fertilizer nitrogen fate in rice fields in the Mekong Delta, Vietnam. Soil Biol. Biochem. 47, 166–174.

Ebrayi, K.N., Pathak, H., Kalra, N., Bhatia, A., Jain, N., 2007. Simulation of nitrogen dynamics in soil using infocrop model. Environ. Monit. Assess. 131 (1–3), 451–465.

Feddes, R.A., Kowalik, P.J., Zaradny, H., 1978. Simulation of Field Water Use and Crop Yield. John Wiley, New York, NY.

Feng, L., Bouman, B., Tuong, T., Cabangon, R., Li, Y., Lu, G., Feng, Y., 2007. Exploring options to grow rice using less water in northern China using a modelling approach I. Field experiments and model evaluation. Agric. Water Manage. 88 (1–3), 1–13.

Garg, K.K., Das, B.S., Safeeq, M., Bhadoria, P.B.S., 2009. Measurement and modeling of soil water regime in a lowland paddy field showing preferential transport. Agric. Water Manage. 96 (12), 1705–1714.

Gaydon, D.S., Probert, M.E., Buresh, R.J., Meinke, H., Timsina, J., 2012. Modelling the role of algae in rice crop nutrition and soil organic carbon maintenance. Eur. J. Agron. 39, 35–43.

Hanson, B.R., Šimůnek, J., Hopmans, J.W., 2006. Evaluation of urea–ammonium–nitrate fertigation with drip irrigation using numerical modeling. Agric. Water Manage. 86 (1–2), 102–113.

Inao, K., Kitamura, Y., 1999. Pesticide paddy field model (PADDY) for predicting pesticide concentrations in water and soil in paddy fields. Pestic. Sci. 55, 38–46.

Janssen, M., Lennartz, B., 2009. Water losses through paddy bunds: methods, experimental data, and simulation studies. J. Hydrol. 369 (1–2), 142–153.

Jeon, J.-H., Yoon, C.G., Ham, J.-H., Jung, K.-W., 2005. Model development for surface drainage loading estimates from paddy rice fields. Paddy Water Environ. 3 (2), 93–101.

Katayanagi, N., Ono, K., Fumoto, T., Mano, M., Miyata, A., Hayashi, K., 2013. Validation of the DNDC-rice model to discover problems in evaluating the nitrogen balance at a paddy-field scale for single-cropping of rice. Nutr. Cycl. Agroecosys. 95 (2), 255–268.

Kyaw, K.M., Toyota, K., Okazaki, M., Motobayashi, T., Tanaka, H., 2005. Nitrogen balance in a paddy field planted with whole crop rice (*Oryza sativa* cv. Kusahonami) during two rice-growing seasons. Biol. Fertil. Soils 42 (1), 72–82.

Li, Y., Barker, R., 2004. Increasing water productivity for paddy irrigation in China. Paddy Water Environ. 2, 187–193.

Lin, X., Zhou, W., Zhu, D., Chen, H., Zhang, Y., 2006. Nitrogen accumulation, remobilization and partitioning in rice (*Oryza sativa* L.) under an improved irrigation practice. Field Crop Res. 96 (2–3), 448–454.

Ling, G., El-Kadi, A.I., 1998. A lumped parameter model for nitrogen transformation in the unsaturated zone. Water Resour. Res. 34 (2), 203–212.

Lotse, E.G., Jabro, J.D., Simmons, K.E., Bakera, D.E., 1992. Simulation of nitrogen dynamics and leaching from arable soils. J. Contam. Hydrol. 10 (3), 183–196.

Mailhol, J.C., Crevoisier, D., Triki, K., 2007. Impact of water application conditions on nitrogen leaching under furrow irrigation: experimental and modelling approaches. Agric. Water Manage. 87 (3), 275–284.

Moya, P., Hong, L., Dawe, D., Chongde, C., 2004. The impact of on-farm water saving irrigation techniques on rice productivity and profitability in Zhanghe Irrigation System, Hubei, China. Paddy Water Environ. 2 (4), 207–215.

Nash, J.E., Sutcliffe, J.V., 1970. River flow forecasting through conceptual models. Part I. A discussion of principles. J. Hydrol. 10 (3), 282–290.

Nguyen Ngoc, M., Dultz, S., Kasbohm, J., 2009. Simulation of retention and transport of copper, lead and zinc in a paddy soil of the Red River Delta, Vietnam. Agric. Ecosyst. Environ. 129 (1–3), 8–16.

Okuda, A., Yamaguchi, M., 1952. Algae and atmospheric nitrogen fixation in paddy soils. II: Relation between the growth of blue-green algae and physical or chemical properties of soil and effect of soil treatments and inoculation on the nitrogen fixation. Mem. Res. Inst. Food Sci. 4, 1–11.

Oulehle, F., Cosby, B.J., Wright, R.F., Hruska, J., Kopacek, J., Kram, P., Evans, C.D., Moldan, F., 2012. Modelling soil nitrogen: the MAGIC model with nitrogen retention linked to carbon turnover using decomposer dynamics. Environ. Pollut. 165, 158–166.

Pachepsky, Y.A., Smettem, K.R.J., Vanderborght, J., Herbst, M., Vereecken, H., Wosten, J.H.M., 2004. Reality and fiction of models and data in soil hydrology. In: Feddes, R.A., et al. (Eds.), Unsaturated Zone Modeling. Kluwer Academic Publishers, Dordrecht.

Pathak, H., Timsina, J., Humphreys, E., Godwin, D.C., Singh, Bijay, Shukla, A.K., Singh, U., Matthews, R.B., 2004. Simulation of rice crop performance and water, nitrogen and carbon dynamics in northwest India using CERES Rice 4.0 model. In: G. CSIRO (Ed.), CSIRO Land and Water Technical Report 23/04. CSIRO Land and Water, NSW 2680, Australia, 111 p.

Patil, M.D., Das, B.S., Bhadoria, P.B.S., 2011. A simple bund plugging technique for improving water productivity in wetland rice. Soil Tillage Res. 112 (1), 66–75.
Patil, M.D., Das, B.S., 2013. Assessing the effect of puddling on preferential flow processes through under bund area of lowland rice field. Soil Tillage Res. 134, 61–71.
Peters, A., Durner, W., 2008. Simplified evaporation method for determining soil hydraulic properties. J. Hydrol. 356 (1–2), 147–162.
Phogat, V., Yadav, A.K., Malik, R.S., Kumar, S., Cox, J., 2010. Simulation of salt and water movement and estimation of water productivity of rice crop irrigated with saline water. Paddy Water Environ. 8 (4), 333–346.
Ramos, T.B., Šimůnek, J., Gonçalves, M.C., Martins, J.C., Prazeres, A., Castanheira, N.L., Pereira, L.S., 2011. Field evaluation of a multicomponent solute transport model in soils irrigated with saline waters. J. Hydrol. 407 (1–4), 129–144.
Ramos, T.B., Šimůnek, J., Gonçalves, M.C., Martins, J.C., Prazeres, A., Pereira, L.S., 2012. Two-dimensional modeling of water and nitrogen fate from sweet sorghum irrigated with fresh and blended saline waters. Agric. Water Manage. 111, 87–104.
Rodrigo, A., Recous, S., Neel, C., Mary, B., 1997. Modelling temperature and moisture effects on C–N transformations in soils: comparison of nine models. Ecol. Model. 102, 325–339.
Roost, N., Cai, X.L., Molden, D., Cui, Y.L., 2008. Adapting to intersectoral transfers in the Zhanghe Irrigation System, China Part I. In-system storage characteristics. Agric. Water Manage. 95 (6), 698–706.
Sander, T., Gerke, H., 2009. Modelling field-data of preferential flow in paddy soil induced by earthworm burrows. J. Contam. Hydrol. 104 (1–4), 126–136.
Šimůnek, J., Hopmans, J.W., 2009. Modeling compensated root water and nutrient uptake. Ecol. Model. 220 (4), 505–521.
Simunek, J., Sejna, M., van Genuchten, M.T., 2008. The HYDRUS-1D software package for simulating the one-dimensional movement of water, heat, and multiple solutes in variably-saturated media. In: Version 4.0. HYDRUS.
Šimůnek, J., Suarez, D.L., 1993. Modeling of carbon dioxide transport and production in soil: 1. Model development. Water Resour. Res. 29 (2), 487–497.
Singh, R., van Dam, J., Jhorar, R.K., 2003. Water and salt balances at farmer fields. In: van Dam, J.C., Malik, R.S. (Eds.), Water Productivity of Irrigated Crops in Sirsa district, India. Integration of Remote Sensing, Crop and Soil Models and Geographical Information Systems. , ⟨http://www.futurewater.nl/downloads/2003_VanDam_WatPro.pdf⟩.
Singh, R., van Dam, J.C., Feddes, R.A., 2006. Water productivity analysis of irrigated crops in Sirsa district, India. Agric. Water Manage. 82 (3), 253–278.
Sun, Y., Ma, J., Sun, Y., Xu, H., Yang, Z., Liu, S., Jia, X., Zheng, H., 2012. The effects of different water and nitrogen managements on yield and nitrogen use efficiency in hybrid rice of China. Field Crop Res. 127, 85–98.
Tan, X., Shao, D., Liu, H., Yang, F., Xiao, C., Yang, H., 2013. Effects of alternate wetting and drying irrigation on percolation and nitrogen leaching in paddy fields. Paddy Water Environ. 11 (1–4), 381–395.
Tan, X., Shao, D., Liu, H., 2014. Simulating soil water regime in lowland paddy fields under different water managements using HYDRUS-1D. Agric. Water Manage. 132, 69–78.
ten Berge, H.F.M., Metselaar, K., Jansen, M.J.W., Agustin, E.M.d.S., Woodhead, T., 1995. The sawah riceland hydrology model. Water Resour. Res. 31 (11), 2721–2732.
Tyagi, N.K., Sharma, D.K., Luthra, S.K., 2000. Determination of evapotranspiration and crop coefficients of rice and sunflower with lysimeter. Agric. Water Manage. 45, 41–54.
Tournebize, J., Watanabe, H., Takagi, K., Nishimura, T., 2006. The development of a coupled model (PCPF-SWMS) to simulate water flow and pollutant transport in Japanese paddy fields. Paddy Water Environ. 4 (1), 39–51.
Tsubo, M., Fukai, S., Basnayake, J., Tuong, T.P., bouman, B., Harnpichitvitaya, D., 2005. Estimating percolation and lateral water flow on sloping land in rainfed lowland rice ecosystem. Plant Prod. Sci. 8 (3), 354–357.
van Genuchten, M., 1980. A closed-form equation for predicting the hydraulic conductivity of unsaturated soils. Soil Sci. Soc. Am. J. 44 (5), 892–898.
Walker, A., 1974. A simulation model for prediction of herbicide persistence. J. Environ. Qual. 3 (4), 296–401.
Wang, H., Ju, X., Wei, Y., Li, B., Zhao, L., Hu, K., 2010. Simulation of bromide and nitrate leaching under heavy rainfall and high-intensity irrigation rates in North China Plain. Agric. Water Manage. 97 (10), 1646–1654.
Watanabe, H., Takagi, K., Vu, S.H., 2006. Simulation of mefenacet concentrations in paddy fields by an improved PCPF-1 model. Pest Manage. Sci. 62 (1), 20–29.
Williams, W.M., Ritter, A.M., Zdinak, C.E., Cheplick, J.M., 1998. RICEWQ—pesticide runoff model for rice crops. In: User's Manual and Program Documentation, Version 1.7.3. Waterborne Environmental, Leesburg, VA.
Yadav, S., Li, T., Humphreys, E., Gill, G., Kukal, S.S., 2011. Evaluation and application of ORYZA2000 for irrigation scheduling of puddled transplanted rice in north west India. Field Crop Res. 122 (2), 104–117.
Yao, F., Huang, J., Cui, K., Nie, L., Xiang, J., Liu, X., Wu, W., Chen, M., Peng, S., 2012. Agronomic performance of high-yielding rice variety grown under alternate wetting and drying irrigation. Field Crop Res. 126, 16–22.
Zhang, L., Lin, S., Bouman, B.A.M., Xue, C., Wei, F., Tao, H., Yang, X., Wang, H., Zhao, D., Dittert, K., 2009. Response of aerobic rice growth and grain yield to N fertilizer at two contrasting sites near Beijing, China. Field Crop Res. 114 (1), 45–53.
Zhang, Z., Zhang, S., Yang, J., Zhang, J., 2008. Yield, grain quality and water use efficiency of rice under non-flooded mulching cultivation. Field Crop Res. 108 (1), 71–81.
Zhao, X., Xie, Y.-X., Xiong, Z.-Q., Yan, X.-Y., Xing, G.-X., Zhu, Z.-l., 2009. Nitrogen fate and environmental consequence in paddy soil under rice-wheat rotation in the Taihu Lake region, China. Plant Soil 319 (1–2), 225–234.
Zhou, S., Nishiyama, K., Watanabe, Y., Hosomi, M., 2008. Nitrogen budget and ammonia volatilization in paddy fields fertilized with liquid cattle waste. Water Air Soil Poll. 201 (1–4), 135–147.